

UC Merced

UC Merced Previously Published Works

Title

Fuels treatment and wildfire effects on runoff from Sierra Nevada mixed-conifer forests

Permalink

<https://escholarship.org/uc/item/8c36q0xj>

Journal

Ecohydrology, 13(3)

ISSN

1936-0584

Authors

Saksa, Philip C
Bales, Roger C
Tague, Christina L
et al.

Publication Date

2020-04-01

DOI

10.1002/eco.2151

Peer reviewed

Fuels treatment and wildfire effects on runoff from Sierra Nevada mixed-conifer forests

P. C. Saksa^{1,5}, R. C. Bales¹, C. L. Tague², J. J. Battles³, B.W. Tobin^{1,4} and M. H. Conklin¹

¹Sierra Nevada Research Institute, University of California, Merced, California, USA. ²Bren School of Environmental Science and Management, University of California, Santa Barbara, California, USA. ³Department of Environmental Science, Policy and Management, University of California, Berkeley, California, USA. ⁴Now at Kentucky Geological Survey, University of Kentucky, Lexington, Kentucky, USA. ⁵Now at Blue Forest, Sacramento, CA, USA.

Corresponding author: Philip Saksa (phil@blueforest.org)

Key Points:

- Relatively light treatments increased runoff in forests with higher precipitation, with greater treatments needed for water-limited forests.
- For light fuels treatments, the water balance in Sierra Nevada forests is sensitive to changes in both forest structure and total biomass.
- Headwater models calibrated with spatially distributed measurements can be scaled to assess hydrologic response in larger catchments

Abstract. We applied an eco-hydrologic model (RHESSys), constrained with spatially distributed field measurements, to assess the impacts of forest-fuels treatments and wildfire on hydrologic fluxes in two Sierra Nevada fireheds. Strategically placed fuels treatments were implemented during 2011-2012 in the upper American River in the central Sierra Nevada (43 km²) and in the upper Fresno River in the southern Sierra Nevada (24 km²). This study used the measured vegetation changes from mechanical treatments and modeled vegetation change from wildfire to determine impacts on the water balance. The well-constrained headwater model was transferred to larger catchments based on geologic and hydrologic similarities. Fuels treatments covered 18% of the American, and 29% of the Lewis catchment. Averaged over the entire catchment, treatments in the wetter central Sierra Nevada resulted in a relatively light vegetation decrease (8%), leading to a 12% runoff increase, averaged over wet and dry years. Wildfire with and without forest treatments reduced vegetation by 38% and 50%, and increased runoff by 55% and 67%, respectively. Treatments in the drier southern Sierra Nevada also reduced the spatially averaged vegetation by 8%, but the runoff response was limited to an increase of less than 3% compared to no treatment. Wildfire following treatments reduced vegetation by 40%, increasing runoff by 13%. Changes to catchment-scale water-balance simulations were more sensitive to canopy cover than to leaf area index, indicating that the pattern as well as amount of vegetation treatment is important to hydrologic response.

Introduction

The risk of damaging wildfire in the Sierra Nevada is increasing (Miller *et al.*, 2009) because of changes in climate (Westerling *et al.*, 2006) and high vegetation densities compared to the previous century (Collins *et al.*, 2011a). There is a need to improve forest resiliency, and thereby mitigate the impact of a changing climate and an altered fire regime, by applying localized integrated management (Stephens *et al.*, 2013). The collective impacts of watershed management, wildfire, and climate will modify the energy and water balance (*e.g.*, evapotranspiration and runoff) in these mountain catchments. As the major source of California's annual water supply, predicting the changes in Sierra Nevada runoff in response to disturbance, forest vegetation management, and growth is a priority (CA Department of Water Resources, 2013).

Fuels treatments can be used in Sierra Nevada mixed-conifer forests to modify the behavior of wildfires (Stephens & Moghaddas, 2005; Stephens, 1998). Runoff response to fuels treatments depends on the pattern and magnitude of prescribed fire (Fernandez *et al.*, 2008; Robichaud, 2000; Robichaud & Waldrop, 1994), shrub removal (Fernandez *et al.*, 2008), and canopy thinning (Robles *et al.*, 2014). The runoff

response to wildfire depends on similar characteristics, such as location in the catchment, fire intensity, and burn severity (Ice *et al.*, 2004). The rate of vegetation regrowth will affect long-term runoff (Hawthorne *et al.*, 2013; Potts *et al.*, 2010). Collins *et al.* (2011b) showed that the effectiveness of fuels treatments was reduced after 20 years of regrowth. Shakesby and Doerr (2006) note that post-fire runoff research at the watershed scale tends to focus on changes to peak flows and erosion potential more than on water yield.

The U.S. Forest Service, the largest land manager in the Sierra Nevada, is incorporating adaptive management into their land-stewardship practices (*e.g.* Bormann *et al.*, 1994, 2007). One of these land-management approaches, Strategically Placed Landscape Treatments (SPLATs; Bahro & Barber, 2004), are fuels treatments designed to disrupt fire paths and reduce overall fire severity. The Sierra Nevada Adaptive Management Project (SNAMP) (Hopkinson & Battles, 2015) was initiated to study the effect of SPLATs on forest health, wildfire, wildlife, and hydrology, with the goal of producing research results that would enable the Forest Service to assess and improve management.

Explicit quantification of water-balance responses to vegetation manipulation is required to fully inform management decisions. Development of novel strategies, such as SPLATs, should incorporate water yield. (Adams, 2013). However, the limited availability of hydrologic observations at the scale relevant to decision making poses a challenge. Prediction and verification tools are needed to transfer observed hydrologic conditions to unmonitored landscapes and projected forest conditions. The application of hydrologic modeling to ungauged catchments has been the subject of much study (Hrachowitz *et al.*, 2013; Sivapalan, 2003; Wagener & Montanari, 2011). One approach for modeling catchments lacking observations has been to transfer model parameters from another instrumented catchment (Bardossy, 2006; Heuvelmans *et al.*, 2004; van der Linden & Woo, 2003). A number of attributes must be considered when regionalizing model parameters from gauged catchments, including spatial proximity, physical similarity, and regression of model parameters and physical characteristics (Merz & Blöschl, 2004; Bao *et al.*, 2012). Studies comparing the methods have noted that parameters of some gauged (donor) catchments can be completely transferred to ungauged (receiver) catchments based on spatial proximity and hydrologic similarity (Kokkonen *et al.*, 2003; Parajka *et al.*, 2005).

The objectives of the study reported here were to: *i*) use the Regional Hydro-Ecologic Simulation System (RHESSys) to integrate data and estimate the effects of implemented SPLATs and modeled wildfires on water balance, *ii*) determine factors controlling landscape-scale hydrologic response to changes in vegetation in water-limited Sierra Nevada forests, and *iii*) assess the transferability of a calibrated headwater-catchment hydrologic model (1-3 km²) to the scales of fire-management projects (firesheds, 20-45 km²).

Methods

This study builds on extensive multidisciplinary research completed in the Tahoe and Sierra National Forests that included vegetation measurement and spatial mapping to assess changes to wildfire behavior with forest-fuels treatments. The study design for the hydrologic component of SNAMP involved intensively monitoring headwater catchments in the American and Merced River basins to develop a watershed-modeling capability that was grounded in distributed observations of snowpack, soil-water storage, and stream discharge (Saksa *et al.*, 2017). We then transferred the calibrated headwater model to assess watershed response to vegetation growth and disturbance to the fireshed that included the headwater catchment. A fireshed, the scale at which forest management is implemented, generally spans tens of km² and is determined by landscape fire characteristics such as regime, history, risk, and

potential behavior (Bahro & Barber, 2004). Fireshed boundaries in this study followed watershed boundaries as part of the integrated design.

Study site and treatments. Each study site in the Tahoe and Sierra National Forests covered three scales of analysis: *i*) headwater catchments for intensive measurement and model development, *ii*) fireshed catchments for assessment of vegetation change on the water balance, and *iii*) a discharge monitoring site downstream from the firesheds for evaluating model transferability from headwater to fireshed. Headwater catchments used for model calibration were Bear Trap Creek (Tahoe NF) and Big Sandy Creek (Sierra NF). Bear Trap (headwater site, 1.4 km², 1620-1825 m elevation) is nested within the American River (fireshed site, 42.9 km², 780-2190 m) and Big Sandy (headwater site, 1.8 km², 1805-2475 m) is adjacent to the Lewis Fork (fireshed site, 24.4 km², 1170-2090 m) (Figure 1). Streams draining the larger firesheds were not gaged due to the remote and steep terrain. The closest stream-discharge measurements below the firesheds are on the North Fork of the Middle Fork of the American R. (downstream site, 230.2 km², 460-2190 m) and on the Lewis Fork of the Fresno R. (downstream site, 42.9 km², 855-2090 m), respectively.

The upper elevations of the American fireshed, including the headwaters, are underlain by Miocene-Pliocene volcanic bedrock; the lower-elevations of the American fireshed are underlain by sedimentary bedrock of the Shoo Fly complex (Saucedo & Wagner, 1992). The bedrock underlying both the Lewis Fork fireshed and Big Sandy headwater consists of plutonic Early Cretaceous Bass Lake Tonalite (Bateman, 1989). Fireshed vegetation transitions from lower-elevation pine-oak to the higher-elevation mixed-conifer forest that covered the headwater sites (Su *et al.*, 2016).

SPLATs were implemented in the fall of 2012 by the local forest districts in accordance with the Record of Decision for the Sierra Nevada Forest Plan Amendment (USFS, 2004), and are hereafter referred to as treatments or vegetation treatments. Vegetation removal was concentrated in 18% and 29% of the American and Lewis study firesheds, respectively (Fry *et al.*, 2015). Fuels treatments consisted of forest thinning by removing a fraction of the trees below 76.2 cm diameter at breast height, mastication and prescribed ground burning. Changes in forest vegetation were determined by differences in Leaf Area Index (LAI), canopy cover, and shrub cover using a combination of LiDAR, color-infrared aerial imagery, and vegetation-plot data collected before and after treatments (Fry *et al.*, 2015; Su *et al.*, 2016).

Vegetation-management scenarios. Four vegetation scenarios were developed from modeling, informed by field measurements: a forest with no treatment and no

fire, a treated forest with no fire, a treated forest followed by fire, and a forest with no treatment followed by fire. Thirty years of vegetation response were modeled for each scenario, based on vegetation growth and fire simulations by Fry *et al.* (2015). Their estimates were developed using the Forest Vegetation Simulator (FVS; Dixon, 2002) with the Fire and Fuels Extension (FFE; Reinhardt & Crookston, 2003), a set of forest-growth models used for calculating forest-stand structure and surface-fuel load over time. A fire-growth model, FARSITE (Finney 2004), was used to simulate wildfire in both the untreated forest and after vegetation treatments were implemented. Wildfire modeled in the American showed that hazardous fire conditions, defined as flame lengths >2 m, covered 33% of the fireshed with no treatment and 23% of the fireshed with treatment. In Lewis Fork, wildfire simulations resulted in hazardous fire conditions over 29% of the fireshed with no treatment and 25% of the fireshed with treatment (Fry *et al.*, 2015). Fire behavior resulting in tree mortality and fuel consumption were used to estimate changes in forest structure.

Four point-in-time snapshots of the modeled vegetation conditions were captured at 0, 10, 20, and 30 years for the two scenarios without wildfire. Forest growth and structure were allowed to stabilize for 10 years following wildfire events, so there were only three snapshots of the vegetation conditions for the two scenarios with wildfire (10, 20, and 30 years). In total, there were 14 point-in-time snapshots of the vegetation conditions across the four vegetation-management scenarios (Table S1). We did not consider short-term responses to fire such as soil hydrophobicity, reduced soil infiltration capacity, and diminished litter cover. These effects are most pronounced immediately after fire. For example, the few studies that address the persistence in soil-water repellence have recorded the effect undetectable within one year (Huffman *et al.*, 2001; MacDonald & Huffman, 2004) to six years after fire (Dyrness, 1976; Henderson & Golding, 1983), although the impact and persistence of hydrophobicity generally increased with burn severity.

RHESSys modeling. The Regional Hydro-Ecologic Simulation System is a spatially distributed, process-based watershed hydrology model that has been widely used to estimate vertical and lateral hydrologic fluxes in snow-dominated mountain environments (e.g. Garcia & Tague, 2015). Previous applications of RHESSys in snow-dominated mountain environments demonstrate that the model can capture daily, seasonal and inter-annual variation in evapotranspiration and streamflow (e.g. Zierl *et al.*, 2007; Bart *et al.*, 2016). The responses of evapotranspiration, surface runoff, and subsurface outflow to vegetation changes were estimated using RHESSys version 5.14.7. RHESSys typically requires

calibration of subsurface-drainage parameters. Calibration in the American was done in the Bear Trap sub-catchment, and in Lewis Fork using the adjacent Big Sandy headwater catchment.

Comprehensive descriptions of the model setup, calibration, and evaluation are described in Saksa *et al.* (2017), and briefly summarized here. In the headwater catchments, the RHESSys model operates at a daily time-step and was driven by regional precipitation measurements from U.S. Bureau of Reclamation stations. Temperature measurements from local upper- and lower-elevation meteorological stations adjacent to the headwaters, were used as input. The separation of precipitation into rain or snow was determined by snow-depth sensors at the stations. Spatially distributed snow-depth and soil-moisture sensors were used to constrain the accumulation and ablation of snowpack over the entire catchment, along with the wetting and drying periods of soil water storage. Stream level was continuously monitored at the stream outlets, and a stage-discharge rating curve was used to calculate daily discharge for model calibration. Calibration used a Monte-Carlo approach described in Tague *et al.* (2013), with six parameter sets meeting minimum calibration criteria for the American and 17 for Lewis Fork (Table S2). Minimum calibration criteria were: *a*) Nash-Sutcliffe Efficiency of daily streamflow > 0.6 , *b*) Nash-Sutcliffe Efficiency of log-transformed daily streamflow > 0.6 , *c*) simulated annual discharge within 20% of measured discharge, *d*) simulated discharge in August within 25% of measured discharge. The criteria were developed to capture both annual and seasonal discharge patterns in a Mediterranean climate. These parameter sets were then transferred directly to the firesheds. We assumed similar hydrologic characteristics between headwaters and firesheds based on subsurface properties and discharge patterns that are detailed below.

Each of the 14 point-in-time snapshots from the four vegetation scenarios described in the previous section were used in RHESSys simulations, with every RHESSys calibration parameter set meeting the minimum calibration criteria, for the four observation years. Mean values of individual water-balance components were calculated from each model simulation and 95% confidence intervals were calculated from the multiple parameter sets to determine statistical significance. In total, there were 84 simulations run for the American (14 scenarios times 6 parameter sets) and 238 simulations run for Lewis Fork (14 scenarios times 17 parameter sets).

For each scenario, the model was run continuously for the four years (2010-2013) of observed precipitation and temperature data. Responses of surface runoff, evapotranspiration, and subsurface outflow were then split into fractions of the total precipitation over the four

years. Surface runoff is the simulated discharge at the stream outlet and evapotranspiration is the sum of evaporation, sublimation, and transpiration. Subsurface outflow is the remaining precipitation not accounted for by runoff and evapotranspiration, including shallow groundwater, deep groundwater, and subsurface water storage within the catchment. Precipitation at each site was obtained from meteorological stations operated by the U.S. Bureau of Reclamation and downloaded from the California Data Exchange Center (CDEC). The Blue Canyon station (1610 m elevation) was used for the American site, and is located 22 km to the northeast of the headwater catchment. The Poison Ridge station (2100 m) was used for the Lewis Fork site, and is located 8 km to the southeast of the headwater catchment. Annual precipitation in the American was 191 cm in 2010, 275 cm in 2011, 160 cm in 2012, and 169 cm in 2013; precipitation in Lewis Fork was 152 cm, 202 cm, 83 cm, and 85 cm for the same years, respectively.

All four years of meteorological observations were used to simulate the hydrologic response for each vegetation scenario, to capture the range of dry to wet precipitation conditions that occurred during this study. These years were representative of long-term climate variability, as precipitation ranged from approximately 60% to 150% of long-term California precipitation indexes (Saksa *et al.*, 2017). Evaluating the hydrologic response over these four years integrates the highly variable climatic conditions typical of the Mediterranean climate in the Sierra Nevada. The model was run for two water years (2008-2009) before each simulation to stabilize the biophysical and hydrologic components. The two-year run allows the vegetation status and hydrologic condition to represent the appropriate environmental conditions at the start of the simulation. For example, if a precipitation event occurred in late 2009 or it was drier than normal for the previous years, it can be accounted for on day one of water year 2010.

Spatially explicit vegetation inputs to RHESSys were obtained from the vegetation map we developed from plot and remote sensing data. The map consisted of stands, or polygons, classified into vegetation types that captured gradients in tree species composition and forest structure. Classification used both multispectral aerial imagery and LIDAR-derived metrics (Su *et al.*, 2016). The forest landscapes were divided into vegetation types. We then used the field-plot data to impute detailed vegetation attributes for each polygon (Fry *et al.*, 2015, Tempel *et al.*, 2015). Key metrics derived from the polygons included overstory Leaf Area Index (LAI), overstory canopy cover, and understory canopy cover. In the American, mean polygon size was 9.7 ha (range: 0.9-72.6 ha) and in the Lewis Fork, mean polygon size was 33.6 ha (3.1-180.7 ha). Overstory LAI

was calculated using allometric relationships (Jones *et al.*, 2015), predicting specific leaf area as function of tree size, species, and vegetation type (Tables S3, S4).

Other than specific leaf area, we used standard ecophysiological parameters for conifer forests from the RHESSys online parameter libraries (Tague and Band, 2004). Understory cover was estimated from forest-plot measurements as a function of overstory cover (Saksa *et al.*, 2017), with understory LAI values determined using the default shrub vegetation parameters in RHESSys. This added element was included because understory vegetation can be an important additional source of transpiration loss following disturbance. The two study sites have different vegetation structures, as determined by the relationship between LAI and canopy cover (Figure 2). In the American catchments, canopy cover increases continuously over the range of mapped LAI values (0-15), attenuating with increases in LAI. In Lewis Fork, canopy cover increases steeply up to a LAI value of 4, with smaller increases above that. Understory cover values were higher in the American (mean = 39%, range = 15-62%) than in Lewis Fork (mean = 28%, range = 1-56%).

Modeling the impact of vegetation on catchment water balance is focused on the following equations (Tague & Band, 2004). LAI is split into sunlit and shaded fractions, based on the photosynthesis model of Chen *et al.* (1999)

$$LAI_{proj_{sunlit}} = 2.0 \times \cos(\theta_{noon}) \times \left\{ 1.0 - \exp^{(-0.5)(1-GF)(LAI_{proj})/\cos(\theta_{noon})} \right\} \quad [1]$$

$$LAI_{proj_{shade}} = LAI_{proj} - LAI_{proj_{sunlit}} \quad [2]$$

where $LAI_{proj_{sunlit}}$ is the projected sunlit LAI, θ_{noon} is the solar angle at noon, GF is the canopy gap fraction, LAI_{proj} is the total LAI, and $LAI_{proj_{shade}}$ is the projected shaded LAI. The canopy gap fraction remained at the default value of zero, as we did not have supporting spatial data to include variable gaps within the canopy, so the projected sunlit and shaded LAI are directly a function of the daily solar angle.

LAI and vegetation cover influence transpiration rates that are estimated using the Penman-Monteith (Monteith, 1965) equation, where stomatal conductance varies as a function of environmental controls, and LAI is used to scale transpiration up to the landscape patch (Equation 3; Jarvis, 1976). The limitations of stomatal conductance for sunlit and shaded canopy were calculated as dimensionless scalar functions (0-1)

$$gs = f(ppfd)f(LWP)f(vpd)(LAI)(gs_{max}) \quad [3]$$

where gs is stomatal conductance ($m s^{-1}$), $f(ppfd)$ is a scalar function of photosynthetic flux density, $f(LWP)$ is a scalar function of leaf-water potential, $f(vpd)$ is a scalar function of vapor-pressure deficit, and gs_{max} is maximum conductance ($m s^{-1}$). The functions for photosynthetic flux density and vapor-pressure deficit

are from Running and Coughlin (1988), and the function for leaf-water potential is in Tague and Band (2004). Plant-water availability in RHESSys is modeled as a function of soil-water potential, a dynamic variable. We assume soil-water potential and predawn leaf-water potential (LWP) are in equilibrium and use LWP in [3] to reduce transpiration under dry conditions.

LAI and vegetation cover also modify snowmelt rates by changing the amount of net surface radiation on the snowpack (Equations 4-6), and by changing canopy interception and sublimation rates. The surface energy balance for snowmelt follows a Beer's law approximation of the amount of incoming shortwave radiation (Equations 4,5), combined with longwave radiation (Equation 6). Incoming direct and diffuse shortwave radiation ($\text{kJ m}^2 \text{ day}^{-1}$) are calculated as

$$K_{direct} = (1 - \alpha_{direct})K_{direct}'\{1 - corr \exp^{-ext_{coef}}\} \quad [4]$$

$$K_{diffuse} = (1 - \alpha_{direct})K_{diffuse}'\{1 - \exp^{-[(1-GF)PAI]^{0.7} + S_c}\} \quad [5]$$

where α_{direct} is the vegetation-specific albedo, K_{direct}' and $K_{diffuse}'$ are the direct and diffuse solar radiation at the top of each vegetation layer, $corr$ is an optional correction factor for low sunlight angles with sparse canopy, ext_{coef} is the Beer's Law extinction coefficient, GF is the gap fraction within the canopy cover, PAI is the plant area index, and S_c is the scattering coefficient. Gap fraction was left at the default value of 0 because we had no data to produce a spatial estimate. Plant area index is based on LAI and adds an estimate of woody biomass for each vegetation type (*e.g.* conifer, deciduous, shrub) to better predict the interception of radiation than using only LAI values (Tague and Band, 2004). If no canopy cover exists, the amount of direct shortwave radiation absorbed by the snowpack is determined by the rate of snow albedo decay from Laramie and Schaake (1972), calculated as

$$\alpha_s = \alpha_0 A^{N^B} \quad [6]$$

where α_s is the snowpack albedo, α_0 is the albedo of new snow, N is the number of days since the last snowfall, and A and B are decay coefficients based on snowpack and temperature conditions (Jost *et al.*, 2009).

Longwave radiation from Croley (1989) was converted to $\text{kJ m}^2 \text{ day}^{-1}$ using the calculation:

$$L = 41.868[ess_{atm}\sigma(T_{air} + 272)^4 - 663] \quad [7]$$

where, ess_{atm} is the emissivity of the atmosphere (Pa), σ is the Stefan-Boltzmann constant ($\text{cal cm}^{-2} \text{ day}^{-1} \text{ K}^4$), and T_{air} is the air temperature ($^{\circ}\text{C}$).

Snowmelt was calculated using a temperature and radiation index model described previously (Saksa *et al.*, 2017). Calibration involved matching the observed daily snowpack patterns from distributed sensors. Although we did not have a similar sensor array at lower elevations in the catchment, the headwater observations overlap with the highest elevations in the

firesheds. The snowpack melt-out date observed at the upper headwater elevations was then used to match the modeled estimate of fireshed-scale snowmelt. Melt-out dates were closest without using any reduction in radiation-driven snowmelt for these simulations.

Results from the wildfire and vegetation growth simulations were translated into the RHESSys vegetation scenarios through modification of the LAI and canopy cover. Because we used specific leaf area to convert canopy bulk density to LAI, and the wildfire and growth simulations have independent methods for estimating changes in canopy cover, it was important to determine the sensitivity of RHESSys to the individual method used to change vegetation in the model. To evaluate the sensitivity of the RHESSys water-balance response to vegetation structure, vertical and horizontal changes in LAI were manipulated separately by changing only LAI or changing only canopy cover over the four years of observation data. These two representations of vegetation change were then compared to the combined LAI and canopy cover changes in the 14 vegetation scenarios. Modifying only LAI changes the vertical structure of vegetation, by increasing or decreasing the density of vegetation on the same area of the watershed. Modifying only canopy cover changes the horizontal structure of the vegetation, increasing or decreasing the fraction of watershed that has forest vegetation or open area, without changing the density of the remaining vegetation cover. In this sensitivity analysis, changes to the canopy cover also modified the LAI, because adjusting the canopy ultimately adds or removes vegetation. LAI and canopy cover were modified from year 0 of the no-treatment scenario, by uniformly multiplying the LAI or canopy cover in each vegetation polygon at 10% increments, from -50% to +60% in the American and from -50% to +20% in Lewis Fork (Table S6). Because of the spatial variation in LAI and canopy cover, and the minimum and maximum values of these vegetation attributes, differences exist in the mean catchment values used for comparison despite the application of a uniform incremental multiplier. For example, a vegetation polygon with 100% canopy cover cannot be increased further.

Model transferability. Within the framework of RHESSys, stream discharge at the outlet of the modeled watershed is normally used to calibrate best-fit subsurface-drainage parameter sets. Tague *et al.* (2013) assessed the ability of RHESSys to function in ungauged catchments, by using geology as a basis for parameter transfer within the same general bioclimatic region. In this study, bedrock geology is similar within the Big Sandy headwater and Lewis Fork fireshed. Both catchments are dominated by the same granodiorite batholith, with less than 1% of each catchment

represented by crystalline metamorphic rock (Bateman, 1989). These geologic units have been assumed to have similar hydrogeologic behavior, with insignificant amounts of water entering deep storage and flowing into streams (Clow *et al.*, 2003).

Bedrock geology in the American study sites also consists of similar compositions between headwater and fireshed. The Bear Trap headwater catchment contains 69% of the Shoo Fly Complex and 31% of volcanic pyroclasts, with the American fireshed having 74% and 26% of the respective geologies. Due to metamorphism, the Shoo Fly Complex can be assumed to be highly crystalline and thus have minimal groundwater flow (Clow *et al.*, 2003). Tague and Grant (2004) have shown that the smaller fraction of volcanic deposits at sites like the American can either have a significant groundwater component or act similarly to crystalline bedrock, depending on the amount of weathering the deposits have experienced. Based on the overall geological similarities, the American headwater being nested within one of the firesheds, and the work of Tague *et al.* (2013), we directly transferred the calibration parameter sets from the headwater models to the fireshed models.

To evaluate these assumptions of geological similarity and direct parameter transfers, discharge from the headwater catchments was compared to discharge data from the closest available sites downstream of the firesheds. In the American, daily discharge from the North Fork of the Middle Fork of the American River (unpublished data, Placer County Water Agency) were used for comparison. In the Lewis Fork, discharge data were available directly downstream (unpublished data, California Department of Water Resources); data from the gauging site were only available for 2012 and 2013. Correlations between headwater and downstream discharge data were calculated as a means of quantifying the similarity between catchments for evaluating model parameter transferability. There is a diversion from Big Creek in the South Fork Merced River catchment that adds water to Lewis Fork during elevated flow periods, generally from November through July. It is assumed that the diversion does not substantially impact the comparison because it is upstream of both the fireshed and the gaged site. Fuels treatments in the firesheds were also implemented in 2011 and 2012, so there may be some influence of treatments in the comparisons. Snowmelt and runoff timing can influence evapotranspiration rates in Sierra watersheds (Tague and Peng, 2013), so annual runoff timing and values were compared between the headwater and downstream gages to assess the direct transfer of flow parameters.

Results

Vegetation scenarios. LAI and canopy cover increased over time in all vegetation-management scenarios in both firesheds (Figures 3a-b, f-g). However, increases in canopy cover were relatively modest in the Lewis Fork because of the high starting values. Treatments only reduced LAI by about 8% in both firesheds (year 0 values on Figures 3a,f), and reduced canopy cover by 9% in the American and 4% in Lewis Fork (year 0 values on Figures 3b,g).

Evapotranspiration increased over the 30-year period in all 4 scenarios in the American but were constant in Lewis Fork (Figures 3c,h). Correspondingly, runoff decreased more in the American than Lewis Fork (Figures 3d,i); decreases in Lewis Fork runoff over time were offset by increases in subsurface outflow instead of evapotranspiration, resulting in almost no net change in total outflow (Figures 3i-j). Increases in both subsurface outflow and evapotranspiration in the American offset decreases in runoff over time (Figures 3d-e).

In the American, vegetation treatments resulted in a small drop in evapotranspiration, with a commensurate increase in the sum of runoff plus subsurface outflow (comparing year 0 values, Figures 3c-e). Net changes with treatment were small in the Lewis Fork (Figures 3h-j). Increases in evapotranspiration and in runoff plus subsurface outflow over the 30-year growth periods in the American were about the same for the no-treatment versus treatment (no fire) scenarios. The increases over 30 years in LAI and canopy cover were also similar for no-treatment versus treatment (Figure 3a-b). Although LAI increased over the 30 years in the Lewis Fork in both scenarios, canopy cover and evapotranspiration did not (Figures 3f-g-h).

In the American fireshed, both fire scenarios show LAI, canopy cover and thus evapotranspiration to be significantly lower after 10, 20 and 30 years compared to the no-fire scenarios (Figures 3a-b-c). For example, vegetation a decade after fire showed 38% and 50% LAI reductions on the treatment and no-treatment landscapes, respectively (Figure 3a). Thus, runoff was significantly higher after fire for both no-treatment and treatment scenarios, with changes in subsurface outflow being much smaller (Figures 3d-e). Note that after 30 years of regrowth, evapotranspiration values and thus the sum of runoff and subsurface outflow, were approaching pre-fire values (Figures 3c-d-e).

In the Lewis Fork, LAI and canopy cover showed qualitatively similar responses to fire as in the American, but evapotranspiration did not change because the canopy-cover and LAI values were still high (Figures 3f-g-h). Similarly, changes in runoff and subsurface outflow with fire offset each other (Figures 3i-j).

Water balance sensitivity to vegetation structure. A sensitivity analysis shows that evapotranspiration and thus runoff is much more sensitive to changes in canopy cover than to changes in LAI, with the Lewis Fork being much less sensitive than the American (Figure 4). Note that the results from Figure 3 are also overlain with sensitivity results on Figure 4. Sensitivity to just LAI, and to LAI plus canopy, were evaluated as indicated on Figures 4d,h. The baseline scenario of no treatment-no fire in the American was a LAI of 7.0 and 56% canopy cover, and in Lewis Fork was a LAI of 9.1 and 77% canopy cover. Note that the response of evapotranspiration, runoff and subsurface flow in the American track the sensitivity-analysis results, for changes in canopy cover (Figures 4a-c). Vegetation treatments (year 0) in the American resulted in a 9% canopy cover decrease, and the magnitude of water-balance response closely matches the 10% decrease in canopy cover in the sensitivity analysis (Figures 4a-d).

In the Lewis catchment, water-balance response to changes in canopy cover are larger in the sensitivity analysis than in the fire and treatment scenarios, reflecting the high values and relatively small changes in canopy cover described above (Figures 4e-h). Evapotranspiration has minimal response to changes in LAI or canopy cover above a LAI value of 8, indicating an upper limit of vegetation impacts on evapotranspiration (Figure 4e). These results are consistent with previous work that has shown that evapotranspiration responses are sensitive to parameters that reflect subsurface storage capacity (Garcia and Tague, 2015).

A sensitivity analysis of the daily water-balance response to $\pm 50\%$ changes in LAI and canopy cover for 2010, an average-precipitation water year, again shows a greater response to vegetation change in the American versus Lewis Fork, reflecting greater water availability and lower vegetation density in the American (Figure 5). As above, changes in canopy cover gave a greater response than did changes in LAI.

The snowpack response to changes in vegetation was minor during the initial accumulation period of December and January, but increased as the winter progressed (Figures 5a,e). Higher snowpack storage occurred with lower LAI and canopy cover, most distinctly at peak snowpack in early- to mid-April. During the spring months of mid-April to June, lower canopy cover resulted in higher snowmelt, and thus less snow accumulation as compared to reducing LAI. Increasing canopy cover by 50% resulted in the slowest snowmelt, and latest melt-out date in the American. Melt-out of snowpack in Lewis fork differed less between the different simulations because of the smaller snowpack, but followed the same trends as the American where snow was most persistent with a reduction in LAI or increase in canopy cover.

Soil-water storage was also more sensitive to changes in canopy cover versus LAI (Figures 5b,f), and is directly linked to the changes in evapotranspiration (Figures 5c,g). Increasing or decreasing LAI had a muted effect on evapotranspiration, indicating that vegetation density in existing canopy cover was not a limiting factor for transpiration. Changes in canopy cover resulted in substantial changes in evapotranspiration, indicating that the presence or absence of vegetation had a larger effect on the water-balance response. Reductions in canopy cover resulted in lower evapotranspiration during winter, spring, and summer. Increased canopy cover resulted in higher evapotranspiration during the same time period, but as noted above increases were limited because some vegetation polygons are already near 100% canopy cover. The lower evapotranspiration with 50% canopy cover resulted in higher soil water storage, most notably in the dry summer and fall periods. Maximum soil-storage values during the winter were more similar in the wetter American than in the drier Lewis Fork, where changes in canopy cover continued to impact soil-water storage through the wet winter season.

The runoff response to changes in vegetation cover are directly linked to the changes in evapotranspiration, and thus are much larger in the American versus Lewis Fork (Figures 5d,h). The 50% increase in LAI also shows an interesting sequence, starting with a lower spring snowpack, which leads to an earlier recession in summer soil-water storage, and results in lower evapotranspiration during the period of maximum energy and water availability (Figure 5c). The opposite occurs with a decrease in LAI: higher spring snowpack, a slower soil-water-storage recession, and higher spring/summer evapotranspiration. This sequence explains why evapotranspiration decreases slightly with the uniformly increasing LAI seen on Figures 4a,e.

Model transferability. The cumulative discharges of headwater and downstream gauged sites for both the American and Lewis Fork catchments exhibit high linear correlation ($R^2 > 0.90$), indicating similar runoff timing between headwater- and fireshed-scale catchments (Figure 6). The firesheds generally have earlier winter runoff and reduced summer baseflow, associated with more rain in the lower elevations. The American fireshed has a lower cumulative runoff fraction than does the headwater (Bear Trap) for the initial 2-6 months of the water year, reflecting greater travel time and subsurface storage in the larger catchment. Annual runoff from the American fireshed catchment was within 25% of the headwater catchments; the fireshed shows a greater variability, with 78% of the headwater runoff in the dry year of 2013 (42 cm) and 119% of headwater runoff in the wet year of 2011 (150 cm). In Lewis Fork, runoff was lower

in both years of available measurements, 2012 (16 cm, 69%) and 2013 (14 cm, 47%), compared to Big Sandy.

Simulations of both American and Lewis Fork fireheds accurately reflected the earlier winter runoff observed in the downstream discharge data, but consistently reported lower annual runoff than in the headwater catchments in each of the four years. In the American, runoff in water year 2010 was substantially underestimated in the model results, and did not reflect the higher runoff observed in the North Fork of the Middle Fork compared to the headwater catchment in 2011. The Lewis Fork model underestimated the observed annual runoff in the 2012 and 2013 water years, but did reflect the lower runoff in the fireshed compared to the measurements in the Big Sandy headwater catchment.

Discussion

Vegetation scenarios. Vegetation disturbance from treatment and fire showed different water-balance responses between the American and Lewis Fork catchments. SPLAT implementation resulted in greater impacts to runoff in the American versus Lewis Fork, and can largely be attributed to the differences in annual precipitation and canopy cover (Figure 2). Changes in vegetation in Lewis Fork had minimal effect on annual evapotranspiration because the forest maintained a higher canopy cover and is more water limited compared to the American, where changes in evapotranspiration were closely linked to canopy cover and forest density. This difference in response can be illustrated using the maximum vegetation change in each catchment, where a 43% vegetation reduction in Lewis Fork (fire, no treatment) led to a 3% decrease in evapotranspiration and a 15% increase in runoff (Figure 5). Alternatively, the maximum 50% vegetation reduction in the American (fire, no treatment) resulted in a 23% decrease in evapotranspiration and a 67% increase in runoff (Figure 3). These modeled changes in LAI from wildfire and regrowth over 30 years are consistent with observations of Roche *et al.* (2018), who evaluated fire effects and regrowth using satellite-derived NDVI.

Evapotranspiration in the American without treatment or fire, was about 115 cm, or 57% of mean annual precipitation (Figure 3c). Roche *et al.* (2018) estimated a lower evapotranspiration of 55-85 cm along the same elevation gradient (800-2200 m) in the same basin. Evapotranspiration in the Lewis Fork without treatment or fire, was about 65 cm, or 50% of the 130-cm mean annual precipitation (Figure 3h). This is comparable to the 50-70 cm of evapotranspiration estimated using a top-down scaling approach based on Normalized Difference Vegetation Index (NDVI), across the same elevation range (1200-2100 m) in the Kings River basin directly south (Goulden *et al.*, 2012).

Using the same top-down approach, Roche *et al.* (2018) showed similar results to those in our study, in that thinning treatments reduced evapotranspiration in the American, but not in the Lewis Fork. More direct evapotranspiration measurements of the wetter and denser forests in northern California are needed to improve verification of this water-balance component.

The impact of changes in forest vegetation on runoff varies by region, forest type, and climate, and by region. Zou *et al.* (2010) use the trend of increasing precipitation with elevation to suggest that vegetation manipulations in the forested upper basin of the Colorado River have greater potential to increase runoff than lower-basin landscapes, using previous forest-thinning studies to propose a 6-25% potential runoff increase. Robles *et al.* (2014) estimated an approximately 20% increase in runoff in thinned forests compared to no thinning in the drier ponderosa pine forests of central Arizona. The estimated increase of runoff following thinning in central Arizona is similar to the runoff response following fire disturbance this study, even with the difference in precipitation.

Forest vegetation growth following treatment or fire disturbance also varies by forest type and disturbance event. Roche *et al.* (2018) found that following wildfire, evapotranspiration in the central Sierra Nevada was reduced at more than double the rate than in the southern Sierra Nevada. Meng *et al.* (2015) showed that vegetation regrowth after fire in a Sierra Nevada mixed-conifer forest was most influenced by fire severity and climate the following year. Ireland and Petropoulos (2015) found similar influences on conifer regrowth in the Ponderosa Pine and Douglas Fir forests of British Columbia, with the most-rapid growth in the first three years after fire. Robles *et al.* (2014) also estimated that runoff increases in Ponderosa Pine forests would be eliminated 6-7 years after thinning, similar to both sites in this study, where runoff increases from thinning were also absent within 10 years of vegetation regrowth. Because external vegetation data were used to provide LAI values to the model in this study, growth scenarios may result in LAI values exceeding what the model would allow given the limited water availability. Further research on forest regeneration and vegetation recovery with respect to hydrologic processes in the Sierra Nevada is needed to evaluate water-balance response following disturbance, given the different water limitations and regrowth rates in the central versus southern Sierra Nevada.

Wildfire impacts on runoff can be greater than thinning, not only from the higher biomass removed, but also from the variability in burn severity, from light understory burns to stand-replacing crown fires. In a central-Arizona ponderosa-pine and mixed-conifer forest, no increases in seasonal or mean annual streamflow were observed after a prescribed burn over

45% of the watershed (Gottfried & DeBano, 1990). Following a stand-replacing fire in central Washington, Helvey (1980) showed that flow rates approximately doubled over the entire flow-duration curve. Simulated fires in the American and Lewis Fork were of mixed severity, and resulted in runoff increases between those reported for prescribed-burn and stand-replacing fires.

Controlling factors of water-balance response to vegetation change. In the American catchments, the water-balance response over the range of vegetation scenarios parallels the pattern of modifying only canopy cover, whereas in the Lewis Fork catchments the water-balance response follows the response to modifying only LAI. The difference in the responses can be attributed to the individual vegetation structures in each catchment, and their relative LAI values. Modifying only canopy cover exerted greater influence on the modeled water balance than modifying only LAI, as evidenced by the higher magnitude of response in evapotranspiration and runoff to changes in the canopy (Figures 3, 4). This reflects the photosynthetic model of Chen *et al.* (1999), where LAI is partitioned into sunlit and shaded portions. The sunlit portion of LAI intercepts most of the photosynthetically active photon-flux density (PPFD), and has the highest potential rate of photosynthesis and transpiration.

When canopy cover is reduced, the amount of sunlit and shaded LAI decreases linearly because any vegetation canopy removal also removes the leaves in that canopy. When LAI values are modified instead, more of the shaded LAI is changed than the sunlit LAI and canopy cover does not change. The sunlit LAI may not change at all if the total LAI exceeds the calculation for sunlit LAI (Equation 1). Thus, the forest structure and method of vegetation change is as important as the magnitude of vegetation differences on the landscape. Model projections often focus specifically on LAI when considering vegetation changes (*i.e.* Running & Nemani, 1991; Tague *et al.*, 2008), but changes in the distribution of vegetation at the patch scale may be more significant than changes in LAI. Additionally, as higher-resolution forest vegetation data become available, capitalizing on the ability of RHESSys to incorporate canopy gap fraction will result in an improved model representation of the heterogeneous forest structure.

Model transferability. Transferring calibrated watershed models to catchments without an available stream gauge remains an active research area, with numerous approaches such as flow duration curve analysis (Zhang *et al.*, 2015), artificial neural networks (Besaw *et al.*, 2010), and similarity of physical watershed characteristics (Clark *et al.*, 2017). The direct transfer of calibrated model parameters has been shown to be an accepted method of simulating nearby

ungauged catchments with similar physiographic characteristics (Kokkonen *et al.*, 2003; Parajka *et al.*, 2005). The headwater and fireshed catchments in this study have similar geologic and vegetation characteristics, but differ in elevation range and catchment size. The lower elevation range in the larger catchments results in more rain with runoff earlier in the year (Figure 3). Lower elevations also had higher evapotranspiration and lower annual runoff compared to higher elevations. This result is consistent with prior observations in the Sierra Nevada where lower-elevation catchments have higher evapotranspiration because of their warmer winter temperatures relative to higher-elevation catchments (Goulden & Bales, 2014). Observations in the American catchments, however, show that the North Fork of the Middle Fork has similar or higher rates of runoff versus the Bear Trap headwater catchment for three out of the four years (Figure 6). Increased winter runoff from greater amounts of precipitation falling as rain may reduce water availability at lower elevations later in the year, when forest water demand is higher (Tague & Peng, 2013). Although many characteristics between the catchments are similar, these differences introduce additional uncertainty to these simulation results. We have explicitly incorporated uncertainty regarding model parameterization, but further research to address the application of different measurement and modeling scales in the Sierra Nevada will be useful in quantifying and constraining this additional uncertainty in model transferability.

Conclusions

The relatively light vegetation changes effected by Strategically Placed Landscape Treatments can increase runoff in the higher-precipitation region of the central-Sierra American River. In the more southern and drier forests represented by the Lewis Fork, however, fuels treatments over a larger portion of the fireshed or a more-intensive treatment may be necessary to measurably change the catchment-scale water balance. The mixed-severity fires modeled in this study also result in even greater vegetation reductions and can lead to large runoff increases.

The representation of forest vegetation structure in hydrologic modeling is important to capture, and will affect predicted impacts of changes in vegetation. Our simulations found that simply accounting for net changes in biomass (represented by LAI) with fuel treatments lead to substantially lower estimates of water-balance impacts than simulations that account for changes in canopy structure (cover). This effect could play an important role when using satellite-data products to interpret vegetation change.

Calibrated watershed models, constrained with observed data, were transferred to ungauged catchments

of similar geology and hydrology to assess watershed response to changes in forest vegetation from growth, treatments, and wildfire. There are a number of uncertainties associated with modeling ungauged catchments, but these uncertainties can be limited by having a well-constrained model in a nearby catchment of similar geologic characterization.

Acknowledgments and Data

We acknowledge the contribution of the Sierra Nevada Adaptive Management Project, an interagency project supported by the USDA Forest Service Region 5, USDA Forest Service Pacific Southwest Research Station, U.S. Fish and Wildlife Service, California Department of Water

Resources, California Department of Fish and Wildlife, California Department of Forestry and Fire Protection, and the Sierra Nevada Conservancy. This is SNAMP publication #58. This research was also supported by the U.S. National Science Foundation, through the Southern Sierra Critical Zone Observatory (EAR-0725097), and a grant from the University of California Division of Agricultural and Natural Resources (11-986). The authors would like to thank the California Department of Water Resources, U.S. Forest Service, Sierra Nevada Research Institute, and Sierra Nevada Adaptive Management Project personnel for their support and assistance. We also thank S. Martin and P. Womble for their significant assistance in fieldwork and data collection. The data used are listed in the references, tables, and online data repository at <https://eng.ucmerced.edu/snsjho>.

References

- Adams, M. A. (2013). Mega-fires, tipping points and ecosystem services: Managing forests and woodlands in an uncertain future. *Forest Ecology and Management*, 294(2013), 250-261. <https://doi.org/10.1016/j.foreco.2012.11.039>.
- Bahro, B., & Barber, K. (2004). Fireshed Assessment: An Integrated Approach to Landscape Planning. *USDA Forest Service Pacific Southwest Region R5-TP-017*.
- Bao, Z., Zhang, J., Liu, J., Fu, G., Wang, G., He, R., & Liu, H. (2012). Comparison of regionalization approaches based on regression and similarity for predictions in ungauged catchments under multiple hydro-climatic conditions. *Journal of Hydrology*, 466-467, 37-46. <https://doi.org/10.1016/j.jhydrol.2012.07.048>.
- Bardossy, A. (2006). Calibration of hydrological model parameters for ungauged catchments. *Hydrology and Earth System Sciences*, 11(2), 703-710. <https://doi.org/10.5194/hessd-3-1105-2006>.
- Bart, R.R., Tague, C.L., Moritz, M.A. (2016). Effect of Tree-to-Shrub Type Conversion in Lower Montane Forests of the Sierra Nevada (USA) on Streamflow. *PLoS ONE*, 11(8). <https://doi.org/10.1371/journal.pone.0161805>.
- Bateman, P. C. (1989). *Geologic Map of the Bass Lake Quadrangle, West-Central Sierra Nevada, California*. Geologic Quadrangle Map GQ-1656. Retrieved from http://ngmdb.usgs.gov/Prodesc/proddesc_28.htm.
- Besaw, L. E., Rizzo, D. M., Bierman, P. R., & Hackett, W. R. (2010). Advances in ungauged streamflow prediction using artificial neural networks. *Journal of Hydrology*, 386(1-4), 27-37. <https://doi.org/10.1016/j.jhydrol.2010.02.037>
- Bormann, B., Cunningham, P., Brooks, M. H., Manning, V. W., & Callopy, M. W. (1994). *Adaptive Ecosystem Management in the Pacific Northwest. General Technical Report* (Vol. PNW-GTR-34). Portland, OR. Retrieved from <http://www.treesearch.fs.fed.us/pubs/8965>.
- Bormann, B. T., Haynes, R. W., & Martin, J. R. (2007). Adaptive Management of Forest Ecosystems: Did Some Rubber Hit the Road? *BioScience*, 57(2), 186. <https://doi.org/10.1641/B570213>.
- California, Department of Water Resources. (2013). *California Water Plan, Update 2013. Bulletin 160-13*. Sacramento, CA.
- Cerda, A., & Doerr, S. H. (2005). The influence of vegetation recovery on soil hydrology and erodibility following fire: an eleven-year investigation. *International Journal of Wildland Fire*, 14(4), 423-437. <https://doi.org/10.1073/WF05044>.
- Chen, J., Liu, J., Cihlar, J., & Goulden, M. (1999). Daily canopy photosynthesis model through temporal and spatial scaling for remote sensing applications. *Ecological Modelling*, 124(2-3), 99-119. [https://doi.org/10.1016/S0304-3800\(99\)00156-8](https://doi.org/10.1016/S0304-3800(99)00156-8).
- Clark, G. E., Ahn, K., & Palmer, R. N. (2017). Assessing a Regression-Based Regionalization Approach to Ungauged Sites with Various Hydrologic Models in a Forested Catchment in the Northeastern United States. *Journal of Hydrologic Engineering*, 22(12), 1-14. [https://doi.org/10.1061/\(ASCE\)HE.1943-5584.0001582](https://doi.org/10.1061/(ASCE)HE.1943-5584.0001582).
- Clow, D. W., Schrott, L., Webb, R., Campbell, D. H., Torizzo, A., & Dornblaser, M. (2003). Ground water occurrence and contributions to streamflow in an alpine catchment, Colorado Front Range. *Groundwater*, 41(7), 937-950. <https://doi.org/10.1111/j.1745-6584.2003.tb02436.x>.
- Collins, B. M., Everett, R. G., & Stephens, S. L. (2011a). Impacts of fire exclusion and recent managed fire on forest structure in old growth Sierra Nevada mixed-conifer forests. *Ecosphere*, 2(4), 14. <https://doi.org/10.1890/ES11-00026.1>.
- Collins, B., Stephens, S., Roller, G., & Battles, J. (2011b). Simulating fire and forest dynamics for a landscape fuel treatment project in the Sierra Nevada. *Forest Science*, 57(2), 77-88. <https://doi.org/10.1093/forestscience/57.2.77>.
- Conklin, M. H., Bales, R. C., Saksa, P. C., Martin, S. E., & Ray, R. (2015). Appendix E: Water Team Final Report in Learning how to apply adaptive management in Sierra Nevada Forests: An integrated assessment (Hopkinson, P., & Battles, J.J., eds.). *Center for Forestry, University of California, Berkeley*, Berkeley, CA. Accessed from <http://snamp.cnr.berkeley.edu/snamp-final-report/index.html>.
- Croley, T. (1989). Verifiable evaporation modeling on the Laurentian Great Lakes. *Water Resources Research*, 25(5), 781-792.
- Dixon, G. E. (2002). Essential FVS: A user's guide to the Forest Vegetation Simulator. *USDA Forest Service, Forest Management Service Center*, 246pp.
- Dyrness, C. T. (1976). Effect of Wildfire on Soil Wettability in the High Cascades of Oregon. *Pacific Northwest Forest and Range Experiment Station* (PNW-202). Portland, OR.

- Fernandez, C., Vega, J., Fonturbel, T., Jimenez, E., & Perez, J. (2008). Immediate effects of prescribed burning, chopping and clearing on runoff, infiltration and erosion in a shrubland area in Galicia (NW Spain). *Land Degradation and Development* 19, 502–515.
- Fry, D., Battles, J., Collins, B., & Stephens, S. (2015). Appendix A - Fire and Forest Ecosystem Health Report in Learning how to apply adaptive management in Sierra Nevada Forests: An integrated assessment (Hopkinson, P., & Battles, J.J., eds.). *Center for Forestry, University of California, Berkeley*, Berkeley, CA. Accessed from <http://snamp.cnr.berkeley.edu/snamp-final-report/index.html>.
- Garcia, E. S., & Tague, C. L. (2015). Subsurface storage capacity influences climate-evapotranspiration interactions in three western United States catchments. *Hydrology and Earth System Sciences*, 19(12), 4845-4858. <https://doi.org/10.5194/hess-19-4845-2015>.
- Gottfried, G. J., & DeBano, L. F. (1990). Streamflow and water quality responses to preharvest prescribed burning in an undisturbed ponderosa pine watershed. *Effects of Fire in Management of Southwestern Natural Resources Conference*, (RM-GTR-191), 222-228. Tuscon, AZ, Nov 14-17, 1988.
- Goulden, M.L., Anderson, R.G., Bales, R.C., Kelley, A.E., Meadows, M. & Winston, G.C. (2012). Evapotranspiration along an elevation gradient in California's Sierra Nevada. *Journal of Geophysical Research*, 117. Doi:10.1029/2012JG002027.
- Goulden, M. L., & Bales, R. C. (2014). Mountain runoff vulnerability to increased evapotranspiration with vegetation expansion. *Proceedings of the National Academy of Sciences*, 1-5. <https://doi.org/10.1073/pnas.1319316111>.
- Hawthorne, S. N. D., Lane, P. N. J., Bren, L. J., & Sims, N. C. (2013). The long term effects of thinning treatments on vegetation structure and water yield. *Forest Ecology and Management*, 310, 983-993. <https://doi.org/10.1016/j.foreco.2013.09.046>.
- Helvey, J. (1980). Effects of a north central Washinton wildfire on runoff and sediment production. *Journal of the American Water Resources Association*, 16(4), 627-634. <https://doi.org/10.1111/j.1753-1688.1980.tb02441.x>.
- Henderson, G. S., & Golding, D. L. (1983). The effect of slash burning on the water repellency of forest soils at Vancouver, British Columbia. *Canadian Journal of Forest Research*, 13, 353-355.
- Heuvelmans, G., Muys, B., & Feyen, J. (2004). Evaluation of hydrological model parameter transferability for simulating the impact of land use on catchment hydrology. *Physics and Chemistry of the Earth, Parts A/B/C*, 29(11-12), 739-747. <https://doi.org/10.1016/j.pce.2004.05.002>.
- Hopkinson, P., & Battles, J. J. (2015). Learning how to apply adaptive management in Sierra Nevada forests : An integrated assessment. *Center for Forestry, University of California, Berkeley*, Berkeley, CA. Accessed from <http://snamp.cnr.berkeley.edu/snamp-final-report/index.html>.
- Hrachowitz, M., Savenije, H. H. G., Blöschl, G., McDonnell, J. J., Sivapalan, M., Pomeroy, J.W., & Cudennec, C. (2013). A decade of Predictions in Ungauged Basins (PUB) – a review. *Hydrological Sciences Journal*, 58(6), 1198-1255. <https://doi.org/10.1080/02626667.2013.803183>.
- Huffman, E. L., MacDonald, L. H., & Stednick, J. D. (2001). Strength and persistence of fire-induced soil hydrophobicity under ponderosa and lodgepole pine, Colorado Front Range. *Hydrological Processes*, 15(15), 2877-2892. <https://doi.org/10.1002/hyp.379>.
- Ice, G., Neary, D., & Adams, P. (2004). Effects of Wildfire on Soils and Watershed Processes. *Journal of Forestry*, 102(6), 16-20. <https://doi.org/10.1093/jof/102.6.16>.
- Ireland, G., & Petropoulos, G. P. (2015). Exploring the relationships between post-fire vegetation regeneration dynamics, topography and burn severity: A case study from the Montane Cordillera Ecozones of Western Canada. *Applied Geography*, 56, 232-248. <https://doi.org/10.1016/j.apgeog.2014.11.016>.
- Jarvis, P. (1976). The interpretation of the variations in leaf water potential and stomatal conductance found in canopies in the field. *Philosophical Transactions of the Royal Society of London*, 273(927), 593-640.
- Jones, D., O'Hara, K., Battles, J., & Gersonde, R. (2015). Leaf Area Prediction Using Three Alternative Sampling Methods for Seven Sierra Nevada Conifer Species. *Forests*, 6(8), 2631-2654. <https://doi.org/10.3390/f6082631>.
- Jost, G., Dan Moore, R., Weiler, M., Gluns, D. R., & Alila, Y. (2009). Use of distributed snow measurements to test and improve a snowmelt model for predicting the effect of forest clear-cutting. *Journal of Hydrology*, 376(1-2), 94-106. <https://doi.org/10.1016/j.jhydrol.2009.07.017>.
- Kokkonen, T. S., Jakeman, A. J., Young, P. C., & Koivusalo, H. J. (2003). Predicting daily flows in ungauged catchments: Model regionalization from catchment descriptors at the Coweeta Hydrologic Laboratory, North Carolina. *Hydrological Processes*, 17(11), 2219-2238. <https://doi.org/10.1002/hyp.1329>.
- Laramie, R. L., & Schaake, J. C. (1972). Simulation of the Continuous Snowmelt Process. *Ralph M. Parsons Laboratory for Water Resources and Hydrodynamics Report 143*, 167 p. Massachusetts Institute of Technology, Cambridge MA.
- MacDonald, L. H., & Huffman, E. L. (2004). Post-fire Soil Water Repellency: Persistence and Soil Moisture Thresholds. *Soil Science Society of America Journal*, 68, 1729-1734. <https://doi.org/10.2136/sssaj2004.1729>.
- Meng, R., Dennison, P. E., Huang, C., Moritz, M. A., & D'Antonio, C. (2015). Effects of fire severity and post-fire climate on short-term vegetation recovery of mixed-conifer and red fir forests in the Sierra Nevada Mountains of California. *Remote Sensing of Environment*, 171, 311-325. <https://doi.org/10.1016/j.rse.2015.10.024>.
- Merz, R., & Blöschl, G. (2004). Regionalisation of catchment model parameters. *Journal of Hydrology*, 287(1-4), 95-123. <https://doi.org/10.1016/j.jhrol.2003.09.028>.
- Miller, J. D., Safford, H. D., Crimmins, M., & Thode, A. E. (2009). Quantitative evidence for increasing forest fire severity in the Sierra Nevada and southern Cascade Mountains, California and Nevada, USA. *Ecosystems*, 12, 16-32. <https://doi.org/10.1007/s10021-008-9201-9>.
- Monteith, J. (1965). Evaporation and the environment. *Proceedings of the 19th Symposium of the Society for Experimental Biology*, Cambridge University Press, 205-233.
- Parajka, J., Merz, R., & Blöschl, G. (2005). A comparison of

- regionalisation methods for catchment model parameters. *Hydrology and Earth System Sciences*, 9, 157-171. <https://doi.org/10.5194/hessd-2-509-2005>.
- Potts, J.B., Marino, E., & Stephens, S.L. (2010). Chaparral shrub recovery after fuel reduction: a comparison of prescribed fire and mastication techniques. *Plant Ecology*, 210(2), 303-315. <https://doi.org/10.1007/s11258-010-9758-1>.
- Robichaud, P. R. (2000). Fire effects on infiltration rates after prescribed fire in Northern Rocky Mountain forests, USA. *Journal of Hydrology*, 231-232, 220-229. [https://doi.org/10.1016/S0022-1694\(00\)00196-7](https://doi.org/10.1016/S0022-1694(00)00196-7).
- Robichaud, P. R., & Waldrop, T. A. (1994). A Comparison of Surface Runoff and Sediment Yields From Low- and High-Severity Site Preparation Burns. *Journal of the American Water Resources Association*, 30(1), 27-34. <https://doi.org/10.1111/j.1752-1688.1994.tb03270.x>.
- Roche, J. W., Goulden, M.L., & Bales, R.C. (2018). Estimating evapotranspiration change due to forest treatment and fire at the basin scale in the Sierra Nevada, California. *Ecohydrology*. 2018;e1978. <https://doi.org/10.1002/eco.1978>.
- Robles, M. D., Marshall, R. M., O'Donnell, F., Smith, E. B., Haney, J. A., & Gori, D. R. (2014). Effects of climate variability and accelerated forest thinning on watershed-scale runoff in southwestern USA ponderosa pine forests. *PloS One*, 9(10), <https://doi.org/10.1371/journal.pone.0111092>.
- Running, S., & Coughlan, J. (1988). A General Model of Forest Ecosystem Processes for regional applications I. Hydrologic balance, canopy gas exchange and primary production processes. *Ecological Modelling*, 42, 125-154.
- Running, S. W., & Nemani, R. R. (1991). Regional hydrologic and carbon balance responses of forests resulting from potential climate change. *Climatic Change*, 19(4), 349-368. <https://doi.org/10.1007/BF00151173>
- Saksa, P., Conklin, M. H., Battles, J. J., Tague, C. L., & Bales, R. C. (2017). Forest thinning impacts on the water balance of Sierra Nevada mixed-conifer headwater basins. *Water Resources Research* 53(7), 5364-5381. <https://doi.org/10.1002/2016WR019240>.
- Saucedo, G. J., & Wagner, D. L. (1992). *Geologic Map of the Chico Quadrangle*. Regional Geologic Map 7A. Retrieved from http://ngmdb.usgs.gov/Prodesc/proddesc_63087.htm.
- Shakesby, R., & Doerr, S. (2006). Wildfire as a hydrological and geomorphological agent. *Earth-Science Reviews*, 74(3-4), 269-307. <https://doi.org/10.1016/j.earscirev.2005.10.006>.
- Sivapalan, M. (2003). Prediction in ungauged basins: a grand challenge for theoretical hydrology. *Hydrological Processes*, 17(15), 3163-3170. <https://doi.org/10.1002/hyp.5155>.
- Stephens, S. L., Agee, J., Fule, P., North, M. P., Romme, W., Swetnam, T., & Turner, M. (2013). Managing Forest and Fire in Changing Climates. *Science*, 342, 41-42. <https://doi.org/10.1126/science.1240294>.
- Stephens, S. L. (1998). Evaluation of the effects of silvicultural and fuels treatments on potential fire behaviour in Sierra Nevada mixed-conifer forests. *Forest Ecology and Management*, 105(1-3), 21-35. [https://doi.org/10.1016/S0378-1127\(97\)00293-4](https://doi.org/10.1016/S0378-1127(97)00293-4).
- Stephens, S. L., & Moghaddas, J. J. (2005). Experimental fuel treatment impacts on forest structure, potential fire behavior, and predicted tree mortality in a California mixed conifer forest. *Forest Ecology and Management*, 215(1-3), 21-36. <https://doi.org/10.1016/j.foreco.2005.03.070>.
- Su, Y., Guo, Q., Fry, D. L., Collins, B. M., Kelly, M., Flanagan, J. P., & Battles, J. J. (2016). A Vegetation Mapping Strategy for Conifer Forests by Combining Airborne LiDAR Data and Aerial Imagery. *Canadian Journal of Remote Sensing*, 42(1), 1-15. <https://doi.org/10.1080/07038992.2016.1131114>.
- Tague, C., & Grant, G. E. (2004). A geological framework for interpreting the low-flow regimes of Cascade streams, Willamette River Basin, Oregon. *Water Resources Research*, 40(4), 1-9. <https://doi.org/10.1029/2003WR002629>.
- Tague, C. L., & Band, L. E. (2004). RHESSys: Regional Hydro-Ecologic Simulation System – An Object-Oriented Approach to Spatially Distribute Modeling of Carbon, Water, and Nutrient Cycling. *Earth Interactions*, 8(19). [https://doi.org/http://dx.doi.org/10.1175/1087-3562\(2004\)8<1:RRHSSO>2.0.CO;2](https://doi.org/http://dx.doi.org/10.1175/1087-3562(2004)8<1:RRHSSO>2.0.CO;2).
- Tague, C. L., Choate, J. S., & Grant, G. (2013). Parameterizing sub-surface drainage with geology to improve modeling streamflow responses to climate in data limited environments. *Hydrology and Earth System Sciences*, 17(1), 341-354. <https://doi.org/10.5194/hess-17-341-2013>.
- Tague, C., & Peng, H. (2013). The sensitivity of forest water use to the timing of precipitation and snowmelt recharge in the California Sierra: Implications for a warming climate. *Journal of Geophysical Research: Biogeosciences*, 118(2), 875-887. <https://doi.org/10.1002/jgrg.20073>.
- Tague, C., Seaby, L., & Hope, A. (2008). Modeling the eco-hydrologic response of a Mediterranean type ecosystem to the combined impacts of projected climate change and altered fire frequencies. *Climatic Change*, 93(1-2), 137-155. <https://doi.org/10.1007/s10584-008-9497-7>.
- Tempel, D.J., Gutierrez, R.J., Battles, J.J., Fry, D.L., Su, Y., Guo, Q., Reetz, M.J., Whitmore, S.A., Jones, G.M., Collins, B.M. & Stephens, S.L. (2015). Evaluating short- and long-term impacts of fuels treatments and simulated wildfire on an old-forest species. *Ecosphere*, 6(12), 1-18. <https://doi.org/10.1890/ES15-00234.1>.
- USFS. (2004). *Sierra Nevada Forest Plan Amendment - Final Supplemental Environmental Impact Statement*. Retrieved from http://www.fs.usda.gov/Internet/FSE_DOCUMENTS/stelprd5416715.pdf.
- van der Linden, S., & Woo, M. (2003). Transferability of hydrological model parameters between basins in data-sparse areas, subarctic Canada. *Journal of Hydrology*, 270(3-4), 182-194. [https://doi.org/10.1016/S022-1694\(02\)00295-0](https://doi.org/10.1016/S022-1694(02)00295-0).
- Wagener, T., & Montanari, A. (2011). Convergence of approaches toward reducing uncertainty in predictions in ungauged basins. *Water Resources Research*, 47(6), 1-8. <https://doi.org/10.1029/2010WR009469>.
- Westerling, A. L., Hidalgo, H. G., Cayan, D. R., & Swetnam, T. W. (2006). Warming and earlier spring increase western U.S. forest wildfire activity. *Science*, 313(5789), 940-3. <https://doi.org/10.1126/science.1128834>.
- Zhang, Y., Vaze, J., Chiew, F. H. S., & Li, M. (2015).

Comparing flow duration curve and rainfall-runoff modelling for predicting daily runoff in ungauged catchments. *Journal of Hydrology*, 525, 72-86. <https://doi.org/10.1016/j.jhydrol.2015.03.043>.

Zierl, B., Bugmann, H., and Tague, C. (2006). Water and carbon fluxes of European ecosystems: an evaluation of the ecohydrological model RHESSys. *Hydrological Processes*,

21(24) 3328-3339. <https://doi.org/10.1002/hyp.6540>.
 Zou, C. B., Ffolliott, P. F., & Wine, M. (2010). Streamflow responses to vegetation manipulations along a gradient of precipitation in the Colorado River Basin. *Forest Ecology and Management*, 259(7), 1268-1276. <https://doi.org/10.1016/j.foreco.2009.08.005>.

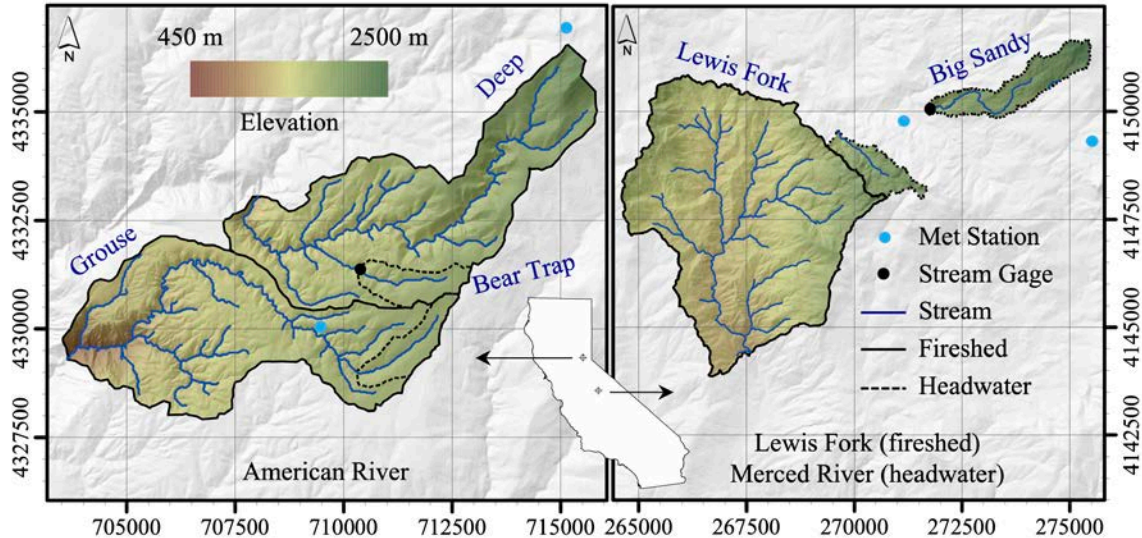


Figure 1. Location of the research catchments, within the American River catchment in Tahoe National Forest (left panel) and Lewis Fork in Sierra National Forest (right panel). Gridlines indicate 2500-m spacing of Universal Transverse Mercator projection; the same elevation shading applies to both maps.

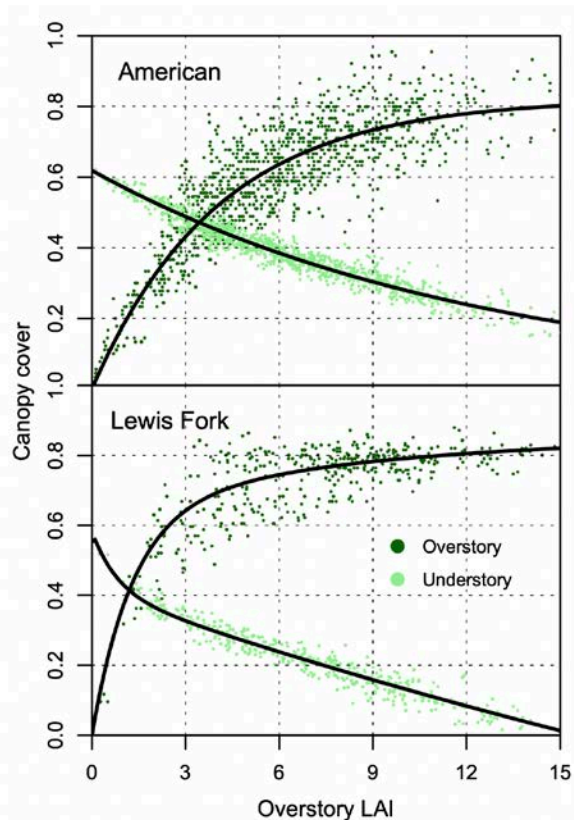


Figure 2. Overstory and understory canopy cover within the range of mapped vegetation overstory leaf area index (LAI) in the no-treatment vegetation maps for the American and Lewis Fork study areas. The vegetation maps input for each scenario modified i) overstory vegetation using both canopy cover and LAI and ii) canopy cover for understory vegetation (no LAI data were available for the understory).

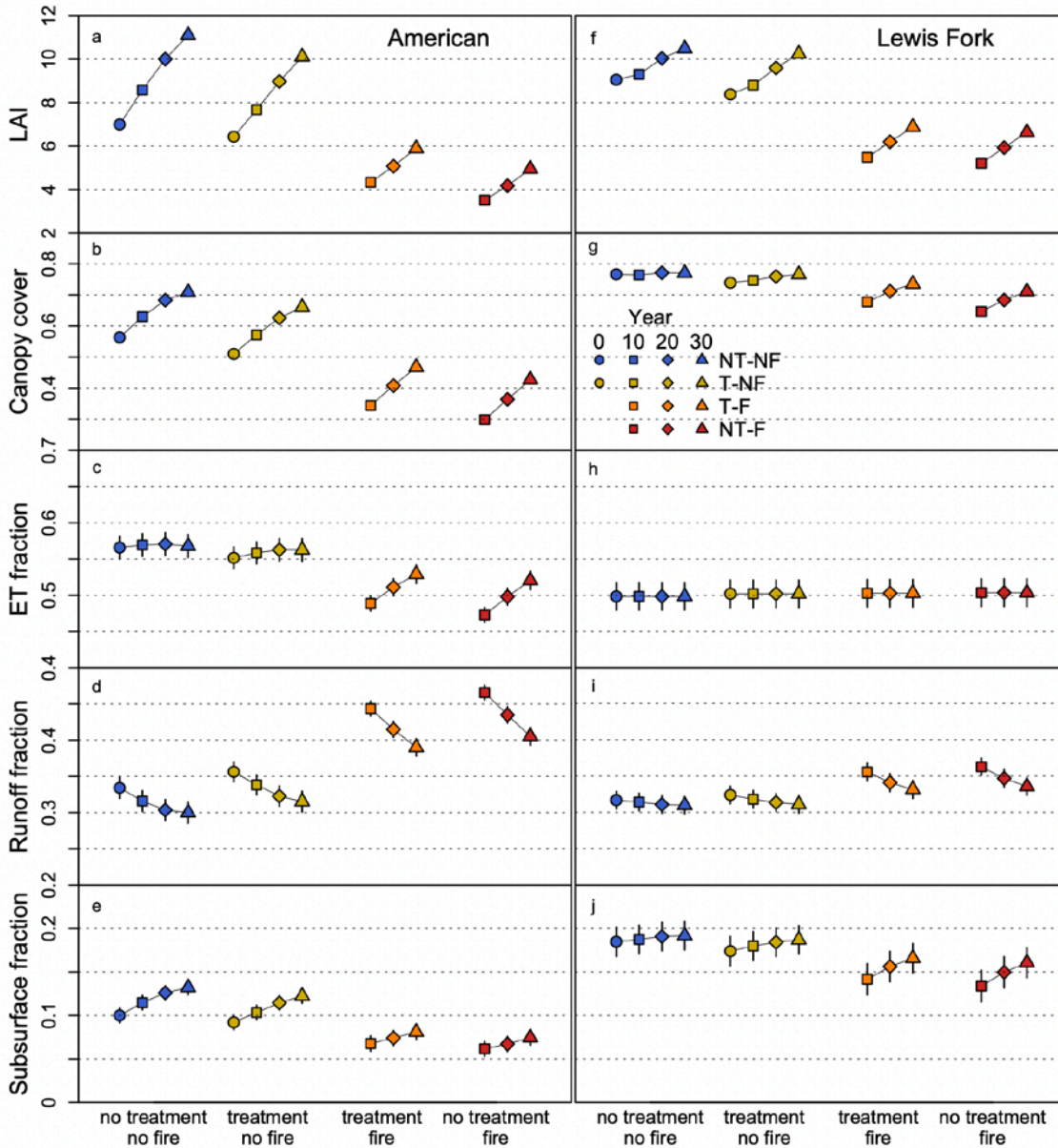


Figure 3. Mean catchment LAI (a,f) and canopy cover (b,g) from simulated management scenarios over 30 years resulted in changes to the partitioning of precipitation into evapotranspiration (c,h), runoff (d,i), and subsurface outflow (e,j). Each water balance component is shown here as a fraction of precipitation, and was modeled over the four years of observed data (water years 2010-2013). Bars indicate 95% confidence intervals, calculated from the multiple model parameter sets, which in some cases is smaller than the symbol size. The four vegetation scenarios are: No Treatment-No Fire (NT-NF), Treatment-No Fire (T- NF), Treatment-Fire (T-F), and No Treatment-Fire (NT-F).

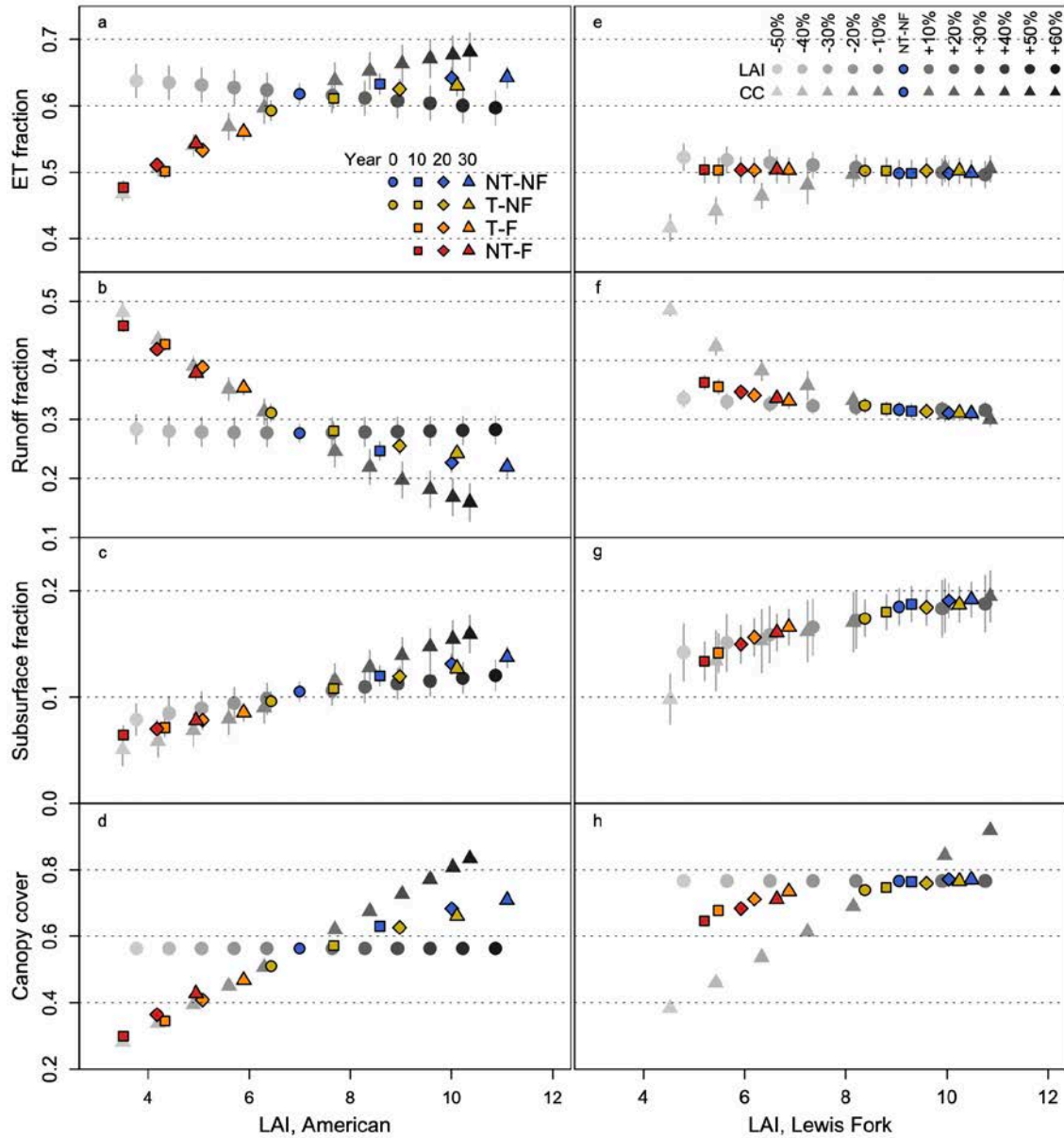


Figure 4. Water-balance response to the vegetation scenarios in Figure 3, compared to uniform changes to leaf area index (LAI) and canopy cover (CC). LAI and CC were increased and decreased in 10% increments, from the no-treatment scenario (blue circles), from 50% to 160% in the American and from 50% to 120% in the Lewis Fork (monochrome symbols). Water-balance components are reported as the fraction of precipitation, averaged over water years 2010-2013. Bars indicate 95% confidence intervals, calculated from the multiple model parameter sets. The four vegetation scenarios are: No Treatment-No Fire (NT-NF), Treatment-No Fire (T-NF), Treatment-Fire (T-F), and No Treatment-Fire (NT-F).

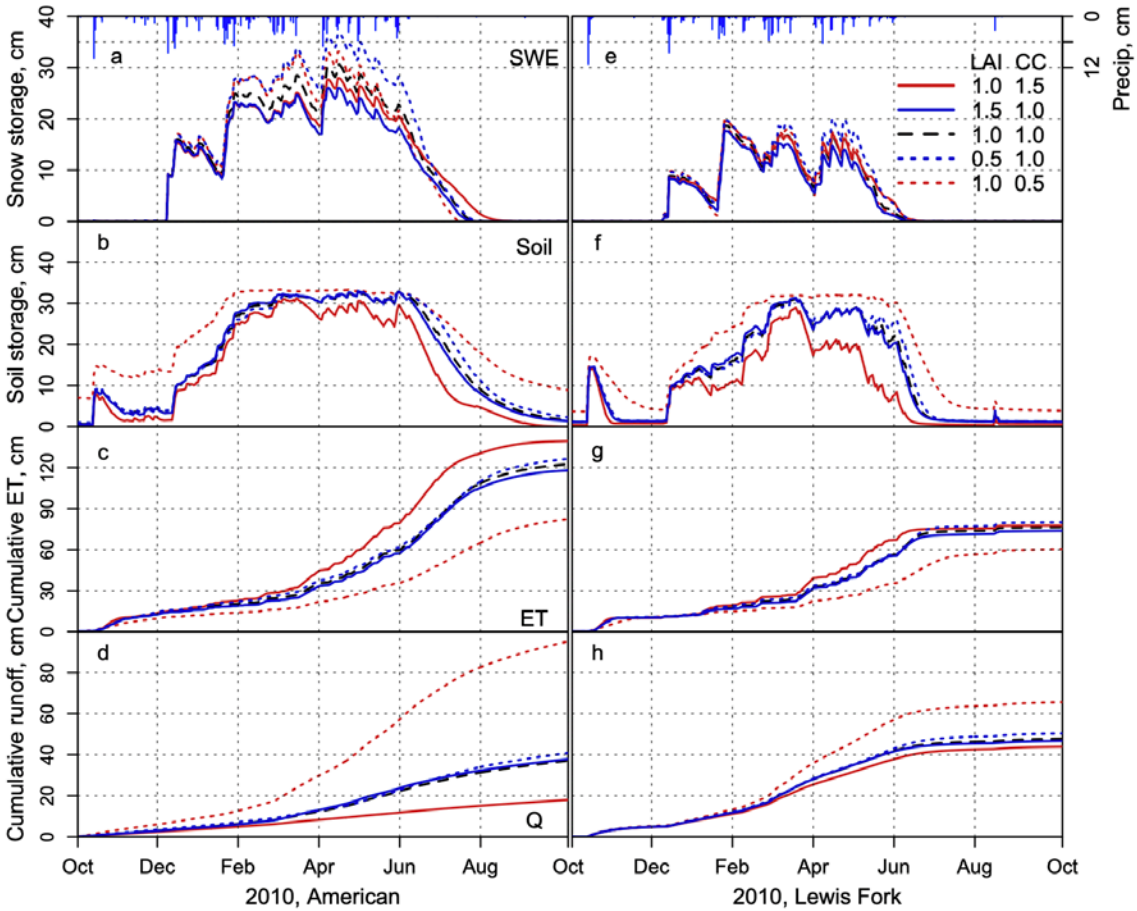


Figure 5. Sensitivity of the daily water-balance to changes in leaf area index (LAI) and canopy cover (CC) for the American (left panel) and Lewis Fork (right panel) freshets in water year 2010. The modeled response of snow water storage (SWE; panels a,e), soil water storage (Soil; panels b,f), evapotranspiration (ET; panels c,g), and runoff (Q; panels d,h) to changing leaf area index or canopy cover by a factor of 0.5 or 1.5 to simulate a 50% decrease or increase from the No treatment-No fire scenario (dashed black line).

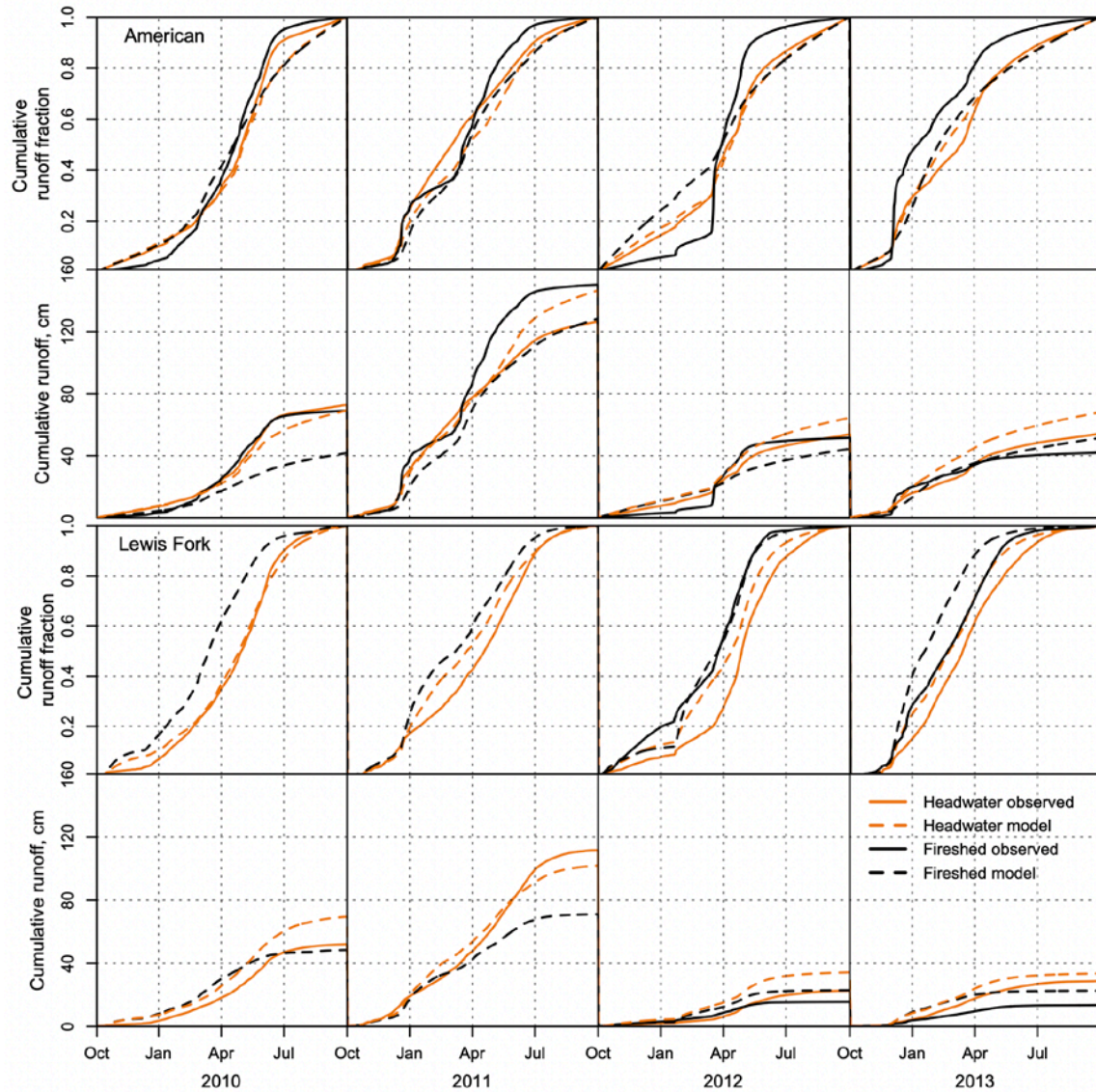


Figure 6. Cumulative discharge of observations and model simulation for the headwater (Bear Trap, Big Sandy) and fireshed (American, Lewis Fork) catchments from 2010 to 2013. Cumulative fractions are used to compare timing of runoff and cumulative runoff normalized over the catchment area is used to compare annual runoff totals. The observation data for Lewis Fork was only available during 2012-2013. American and Lewis Fork observed runoff locations were as close as possible to modeled runoff locations, but would not be expected to be completely aligned because of the different drainage areas.

Table S1. The four management scenarios and point-in-time snapshots of vegetation conditions resulting in a total of 14 scenarios used in this study. The “No Fire” scenarios have 4 point-in-time snapshots over 30 years (year 0, 10, 20, 30). The “Fire” scenarios have 3 point-in-time snapshots over 20 years (year 10, 20, 30), because vegetation was allowed to grow and stabilize for 10 years following the wildfire event.

Vegetation Scenarios	Year 0	Year 10	Year 20	Year 30
No Treatment – No Fire (NT-NF)	x	x	x	x
Treatment – No Fire (T-NF)	x	x	x	x
Treatment – Fire (T-F)		x	x	x
No Treatment – Fire (NT-F)		x	x	x

Table S2. The RHESys parameters used to model the American (6 sets) and Lewis Fork (17 sets) catchments.^a

American

<i>hk</i>	<i>vk</i>	<i>m</i>	<i>po</i>	<i>pa</i>	<i>gw1</i>	<i>gw2</i>
5.98	58.61	5.67	2.54	1.81	0.06	0.004
6.55	232.56	11.73	2.40	2.26	0.15	0.008
5.13	206.00	6.25	2.91	1.06	0.05	0.002
3.86	7.05	6.14	1.47	0.60	0.14	0.003
2.07	249.87	12.30	1.83	2.57	0.05	0.003
3.20	146.73	7.82	1.57	0.60	0.08	0.010

Lewis Fork

<i>hk</i>	<i>vk</i>	<i>hm</i>	<i>po</i>	<i>pa</i>	<i>gw1</i>	<i>gw2</i>
92.39	286.48	0.96	0.22	2.85	0.24	0.38
21.27	192.10	2.63	2.80	0.95	0.24	0.17
135.08	40.93	4.03	1.17	2.44	0.36	0.35
239.90	2.88	0.67	0.43	0.82	0.35	0.33
293.75	103.25	6.17	2.12	1.42	0.34	0.34
4.80	293.34	4.44	0.90	1.65	0.26	0.28
203.09	39.32	1.26	2.18	2.68	0.40	0.33
97.00	154.41	5.13	1.04	0.24	0.40	0.21
249.05	233.83	7.94	1.49	0.32	0.30	0.34
73.09	266.66	6.93	2.50	2.24	0.30	0.30
219.32	288.06	17.64	0.75	2.78	0.38	0.25
7.50	195.53	18.2	0.73	1.63	0.39	0.29
28.74	237.23	9.9	2.98	1.60	0.32	0.17
252.44	200.75	7.39	2.00	0.52	0.31	0.26
98.43	176.68	7.27	0.30	1.48	0.38	0.22
51.11	130.96	19.94	0.11	1.44	0.32	0.16
173.89	91.41	16.92	1.16	2.16	0.39	0.28

^aThe multiple parameter sets were used to calculate a 95% confidence interval for every simulated vegetation scenario. The parameters are lateral hydraulic conductivity (*hk*), vertical hydraulic conductivity (*vk*), and decay of hydraulic conductivity with depth (*vm*), percent of infiltrated water routed to deep groundwater (*gw1*), deep-groundwater drainage (*gw2*), and soil physical properties of pore-size index (*po*) and air-entry pressure (*pa*).

Table S3. Tree species composition of the vegetation community types in the American^a.

Species	SLA, m ² kg ⁻¹	Species contribution to forest type, percent				
		true fir forest, open	pine-fir forest, sparse cover	cedar-white fir mixed conifer forest, medium cover	mixed conifer forest, medium cover	mixed conifer forest, high cover
<i>Abies concolor</i>	8.0	37	25	39	25	34
<i>Abies magnifica</i>	6.7	19	15	1	1	5
<i>Calocedrus decurrens</i>	8.9	0	0	12	9	8
<i>Cornus nuttallii</i>	32.0	0	0	0	0	0
<i>Quercus agrifolia</i>	32.0	0	0	0	0	0
<i>Pinus lambertiana</i>	11.1	0	16	17	20	20
<i>Pinus monticola</i>	11.1	6	2	0	0	0
<i>Pseudotsuga menziesii</i>	12.2	17	16	15	20	19
<i>Pinus ponderosa</i>	8.1	21	26	14	23	11
<i>Quercus kelloggii</i>	32.0	0	0	1	2	3
<i>Sequoiadendron giganteum</i>	8.9	0	0	1	0	0
		Aggregate quantities				
SLA weighted mean, m ² kg ⁻¹		8.7	9.0	9.3	10.1	10.1
Fraction		0.390	0.384	0.480	0.458	0.562
Basal area, m ² ha ⁻¹		2.2	10.4	17.1	24.3	45.1
Percent of Area		1.7	2.7	5.4	5.9	84.3

^aSpecific Leaf Area (SLA) of each species is also given and used with the percent basal area of each species to calculate SLA for each community type, similar to Jones *et al.* (2015). Percent basal area of each species was determined from field vegetation plots (Fry *et al.*, 2015).

Table S4. Tree species composition of the vegetation community types in the Lewis Fork^a.

Species	SLA, m ² kg ⁻¹	Species contribution to forest type, percent			
		Open pine- oak woodland	live oak-pine forest	mature mixed conifer forest	closed-canopy mixed conifer forest
<i>Abies concolor</i>	8.0	0	0	26	28
<i>Calocedrus decurrens</i>	8.9	0	4	33	39
<i>Pinus lambertiana</i>	11.1	0	0	9	16
<i>Pinus ponderosa</i>	8.1	51	30	18	13
<i>Quercus kelloggii</i>	32.0	49	10	9	3
<i>Quercus wislizeni</i>	32.0	0	43	0	0
		Aggregate quantities			
SLA weighted mean, m ² kg ⁻¹		19.8	19.7	10.4	9.5
fraction		0.173	0.436	0.677	0.8
Basal area, m ² ha ⁻¹		11.6	12.9	48	80.2
Percent of Area		0.0	5.9	88.2	5.9

^aSpecific Leaf Area (SLA) of each species is also given and used with the percent basal area of each species to calculate SLA for each community type, similar to Jones *et al.* (2015). Percent basal area of each species was determined from field vegetation plots (Fry *et al.*, 2015).

Table S5. Changes in the partitioning of precipitation into evapotranspiration (ET), runoff (Q), and subsurface outflow (Sub) in response to changes in mean leaf area index (LAI) and canopy cover (CC) of simulated management scenarios over 30 years.^a

American Year	No treatment-No fire				Treatment-No fire				Treatment-Fire			No treatment-Fire		
	0	10	20	30	0	10	20	30	10	20	30	10	20	30
ET	0.618 (0.025)	0.633 (0.025)	0.642 (0.026)	0.643 (0.026)	0.593 (0.024)	0.611 (0.024)	0.625 (0.025)	0.630 (0.025)	0.501 (0.017)	0.533 (0.019)	0.561 (0.020)	0.477 (0.017)	0.511 (0.019)	0.543 (0.020)
Q	0.277 (0.025)	0.247 (0.026)	0.227 (0.027)	0.220 (0.027)	0.311 (0.024)	0.281 (0.024)	0.255 (0.025)	0.243 (0.026)	0.428 (0.017)	0.389 (0.019)	0.354 (0.019)	0.459 (0.017)	0.419 (0.018)	0.379 (0.020)
Sub	0.105 (0.009)	0.120 (0.009)	0.131 (0.009)	0.137 (0.010)	0.096 (0.009)	0.108 (0.009)	0.119 (0.009)	0.127 (0.009)	0.071 (0.009)	0.078 (0.009)	0.085 (0.009)	0.064 (0.009)	0.070 (0.009)	0.078 (0.009)
LAI	6.995	8.583	10.004	11.099	6.432	7.670	8.975	10.108	4.333	5.077	5.891	3.511	4.176	4.948
CC	0.563	0.630	0.683	0.708	0.510	0.571	0.626	0.660	0.344	0.408	0.468	0.299	0.364	0.427

Lewis Fork Year	No Treatment-No Fire				Treatment-No Fire				Treatment-Fire			No treatment-Fire		
	0	10	20	30	0	10	20	30	10	20	30	10	20	30
ET	0.498 (0.019)	0.498 (0.019)	0.498 (0.019)	0.498 (0.019)	0.496 (0.019)	0.496 (0.019)	0.496 (0.019)	0.496 (0.019)	0.497 (0.019)	0.497 (0.019)	0.497 (0.019)	0.499 (0.019)	0.499 (0.019)	0.499 (0.019)
Q	0.317 (0.012)	0.315 (0.012)	0.311 (0.012)	0.310 (0.012)	0.325 (0.012)	0.319 (0.012)	0.314 (0.012)	0.311 (0.012)	0.358 (0.012)	0.343 (0.012)	0.333 (0.012)	0.365 (0.012)	0.349 (0.012)	0.337 (0.012)
Sub	0.185 (0.017)	0.187 (0.017)	0.190 (0.017)	0.191 (0.017)	0.179 (0.018)	0.185 (0.018)	0.190 (0.017)	0.193 (0.017)	0.145 (0.019)	0.160 (0.018)	0.170 (0.018)	0.137 (0.019)	0.153 (0.019)	0.164 (0.018)
LAI	9.053	9.299	10.037	10.484	8.378	8.800	9.596	10.245	5.481	6.193	6.875	5.205	5.928	6.637
CC	0.766	0.764	0.771	0.770	0.739	0.747	0.759	0.766	0.677	0.712	0.735	0.646	0.483	0.711

^aEach water balance component is shown here as a fraction of precipitation, and was modeled over the four years of observed data (water years 2010-2013). The values in this table correspond to the values in Figure 3; values in parentheses are 95% confidence intervals, calculated from the multiple model parameter sets.

Table S6. Scenarios used for the model sensitivity analysis. Both Leaf Area Index (LAI) and Canopy Cover (CC) were manually adjusted from the No Treatment – No Fire (NT-NF, Year 0) scenario to determine the controlling factors of vegetation structure on hydrologic response. The 100% LAI and CC scenarios are the same as in the original NT-NF scenario. In the American, LAI and CC are decreased to 50% of the NT-NF scenario, and increased up to a maximum of 160% of NT-NF. In the Lewis Fork, LAI and CC are decreased to 50% of the NT-NF scenario, and increased up to a maximum of 120% of NT-NF. The differences in increased LAI and CC between the catchments reflects the individual range of these values in all 14 modeled scenarios.

American No Treatment – No Fire Year 0 Leaf Area Index (LAI)	American No Treatment – No Fire Year 0 Canopy Cover (CC)	Lewis Fork No Treatment – No Fire Year 0 Leaf Area Index (LAI)	Lewis Fork No Treatment – No Fire Year 0 Canopy Cover (CC)
LAI x 160%	CC x 160%		
LAI x 150%	CC x 150%		
LAI x 140%	CC x 140%		
LAI x 130%	CC x 130%		
LAI x 120%	CC x 120%	LAI x 120%	CC x 120%
LAI x 110%	CC x 110%	LAI x 110%	CC x 110%
LAI x 100%	CC x 100%	LAI x 100%	CC x 100%
CC x 90%	CC x 90%	CC x 90%	CC x 90%
CC x 80%	CC x 80%	CC x 80%	CC x 80%
CC x 70%	CC x 70%	CC x 70%	CC x 70%
CC x 60%	CC x 60%	CC x 60%	CC x 60%
CC x 50%	CC x 50%	CC x 50%	CC x 50%